

A Hybrid MMSE and K-Best Detection Scheme for MIMO Systems

Cheng-Yu Hung, Ronald Y. Chang, and Wei-Ho Chung*

Research Center for Information Technology Innovation, Academia Sinica, Taiwan

*E-mail: whc@citi.sinica.edu.tw

Abstract—A new multiple-input multiple-output (MIMO) detection scheme combining minimum-mean-square-error (MMSE) detection and the K-best detection algorithm is proposed. The proposed scheme leverages the MMSE detection results to ease the demand of a large K in the conventional K-best algorithm to achieve satisfactory performance. The post-detection SNR obtained after MMSE detection is consulted to determine the symbols upon which a reduced-dimension K-best algorithm (*h*-best algorithm) is performed to obtain final detection results. Parameters associated with the proposed scheme are empirically chosen to make a fair comparison with the conventional K-best algorithm. Extensive Monte Carlo simulation demonstrates that the hybrid approach exhibits significant performance gain over both MMSE and K-best detection schemes.

Index Terms—MIMO systems, maximum likelihood detection, MMSE detection, K-best detection algorithm.

I. INTRODUCTION

The multiple-input multiple-output (MIMO) technique has attracted numerous research interests in the area of wireless communications due to its capability of providing high data rates (spatial multiplexing) and/or enhanced reliability (diversity). One of the major challenges of employing the MIMO technique lies in the detector design, which decouples the transmitted signal that has been mixed by the MIMO channel at the receiving end. Towards this end, ML detection is theoretically optimal, but its prohibitively high computational complexity forbids its practical use.

Due to the infeasibility of ML detection in practice, many optimal and suboptimal detection algorithms have been proposed, such as the sphere decoder (SD) [1], K-best algorithm [2], zero-forcing (ZF) detector, MMSE detector, and ordered successive interference cancellation (OSIC). The original SD [3] uses a depth-first tree search to find a solution by searching all lattice points within a sphere radius. Based on a zigzag search method inside the sphere, a reduced-complexity version of SD was introduced by Schnorr and Euchner [4]. The K-best algorithm [5]–[8] conducts a breadth-first tree search to find a suboptimal solution. The K-best algorithm retains K nodes at each layer before proceeding to the next layer so that its complexity is fixed and is more suitable for hardware implementation. Linear equalizers, including the ZF detector [9] and MMSE detector [10], have very low complexity at the cost of some performance and diversity loss. The OSIC

scheme [11] detects symbols in descending order of their post-detection signal-to-noise ratio (SNR). The contribution of a detected symbol is then subtracted from the received signal before detecting the next symbol. The Markov chain Monte Carlo (MCMC) technique [12] executes the Gibbs sampling (GS) procedure to generate a list of likely candidates of transmitted symbol vectors for detection. By reducing the search set, the multilevel detection scheme [13] achieves near-ML performance with much lower complexity.

In this paper, we propose a novel hybrid MIMO detection scheme that leverages the low-complexity advantage of MMSE detection and the fixed-complexity characteristics of the K-best detection algorithm. The proposed scheme first performs standard MMSE detection, followed by reduced-dimension K-best detection applied on selected symbols based on the MMSE detection results. Specifically, all symbols associated with lower post-detection SNR (in the error-layer group) and few selected symbols associated with higher post-detection SNR (in the correct-layer group) are jointly detected by a *h*-best algorithm¹. The proposed scheme is demonstrated by computer simulation to achieve superior symbol error rate (SER) performance (as much as 8 dB gain) over conventional K-best algorithm, at comparable complexity cost.

The rest of this paper is organized as follows. The system model and related MIMO detection algorithms are briefly introduced in Sec. II. In Sec. III, the proposed hybrid scheme based on MMSE detection and the K-best algorithm is described and the computational complexity is evaluated. Simulation results are presented in Sec. IV. Concluding remarks are given in Sec. V.

Notations: In this paper, vectors and matrices are set in boldface, with lowercase and uppercase letters representing vectors and matrices, respectively. \mathbf{I}_M represents the $M \times M$ identity matrix. $\|\cdot\|$ denotes the l_2 -norm of a vector. The $(\cdot)^{-1}$, $(\cdot)^T$ and $(\cdot)^H$ represent matrix inverse, matrix transpose and Hermitian matrix transpose, respectively. $\mathbb{E}[\cdot]$ denotes expectation, and $[\cdot]_S$ represents quantization (slicing) with respect to the set S .

This work was supported by the National Science Council of Taiwan under Grant NSC 100-2221-E-001-004.

¹A reduced-dimension K-best algorithm is specifically termed the *h*-best algorithm ($h < K$) in this paper to differentiate it from the conventional K-best algorithm.

II. SYSTEM MODEL AND REVIEW OF RELATED DETECTION SCHEMES

A. MIMO System Model and ML Detection

The MIMO system with M_T transmit antennas and M_R receive antennas ($M_R \geq M_T$) is considered. The baseband signal can be modeled as

$$\mathbf{y} = \mathbf{H}\mathbf{x} + \mathbf{v} \quad (1)$$

where \mathbf{y} denotes the $M_R \times 1$ received complex symbol vector, \mathbf{x} denotes the $M_T \times 1$ transmitted complex symbol vector that contains uncorrelated entries from the countably finite modulation alphabet \mathcal{S} and has zero mean and covariance matrix $\sigma_x^2 \mathbf{I}_{M_T}$, \mathbf{H} denotes the $M_R \times M_T$ Rayleigh fading channel matrix which has independent and identically distributed (i.i.d.) complex-valued Gaussian entries with zero mean and covariance matrix \mathbf{I}_{M_R} , and \mathbf{v} denotes the additive white Gaussian noise (AWGN) vector with zero mean and covariance matrix $\sigma_v^2 \mathbf{I}_{M_R}$. We assume that the channel matrix \mathbf{H} is perfectly known at the receiver and $M_R = M_T$.

Based on the system model in (1), ML detection of the transmitted symbol vector is given by [14]

$$\tilde{\mathbf{x}}_{\text{ML}} = \arg \min_{\mathbf{x} \in \mathcal{S}^{M_T}} \|\mathbf{y} - \mathbf{H}\mathbf{x}\|^2. \quad (2)$$

ML detection is optimal in the sense that it finds a solution that minimizes the error probability given equally probable transmitted symbol vectors. However, a major drawback of ML detection is its prohibitively high computational complexity due to exhaustive search over the space \mathcal{S}^{M_T} .

B. Linear Detection

Two linear detection schemes that have extremely low complexity, namely, ZF and MMSE equalizers, are reviewed here. The ZF equalization matrix \mathbf{G}_{ZF} is given by the Moore-Penrose pseudo-inverse of \mathbf{H} [15]:

$$\mathbf{G}_{\text{ZF}} = (\mathbf{H}^H \mathbf{H})^{-1} \mathbf{H}^H. \quad (3)$$

The MMSE equalization matrix, derived by minimizing the mean square error $\mathbb{E}[\|\mathbf{G}\mathbf{y} - \mathbf{x}\|^2]$, is given by [14]

$$\mathbf{G}_{\text{MMSE}} = (\mathbf{H}^H \mathbf{H} + (\sigma_v^2 / \sigma_x^2) \mathbf{I}_{M_T})^{-1} \mathbf{H}^H. \quad (4)$$

The ZF and MMSE equalization outputs are

$$\hat{\mathbf{x}}_{\text{ZF}} = \mathbf{G}_{\text{ZF}} \mathbf{y} = (\mathbf{H}^H \mathbf{H})^{-1} \mathbf{H}^H \mathbf{y} \quad (5)$$

$$\begin{aligned} \hat{\mathbf{x}}_{\text{MMSE}} &= \mathbf{G}_{\text{MMSE}} \mathbf{y} \\ &= (\mathbf{H}^H \mathbf{H} + (\sigma_v^2 / \sigma_x^2) \mathbf{I}_{M_T})^{-1} \mathbf{H}^H \mathbf{y}. \end{aligned} \quad (6)$$

The detected symbol vectors are generated through the quantization operation $[\cdot]_{\mathcal{S}}$. The ZF detected symbol vector is $\tilde{\mathbf{x}}_{\text{ZF}} = [\hat{\mathbf{x}}_{\text{ZF}}]_{\mathcal{S}}$ and the MMSE detected symbol vector is $\tilde{\mathbf{x}}_{\text{MMSE}} = [\hat{\mathbf{x}}_{\text{MMSE}}]_{\mathcal{S}}$.

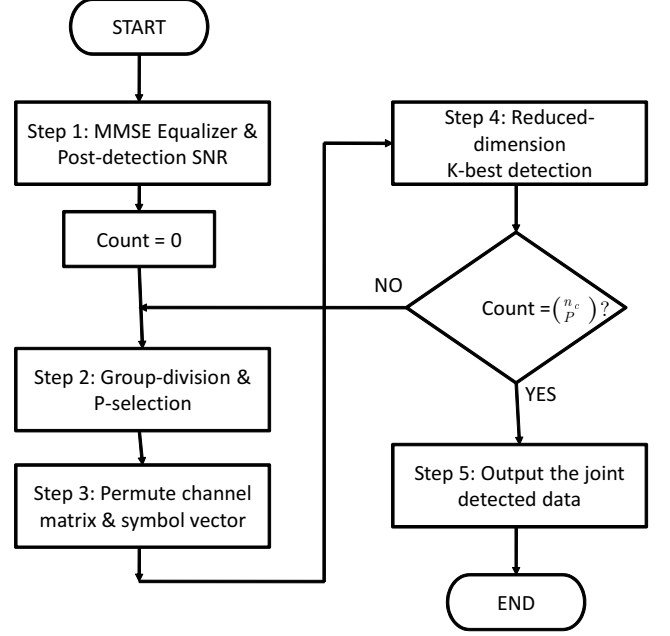


Fig. 1. Flowchart of the proposed hybrid MMSE and K-best detection.

C. K-best Detection

The K-best detection algorithm [7] performs breadth-first tree search by retaining only K nodes with the smallest accumulated partial Euclidean distance (PED) at each detection layer until the leaf nodes are reached. The K-best algorithm is implementation-friendly due to its constant throughput. However, it has two fundamental issues: 1) the choice of K is a tradeoff between performance and complexity, and in the case of large K , the complexity is quite high due to more operations needed to calculate and sort the PEDs; 2) in high SNR regime, the K-best algorithm is observed to be impacted by the error floor.

III. THE PROPOSED HYBRID MMSE AND K-BEST DETECTION

Motivated by the observation that the complexity of the K-best algorithm may be further reduced with the aid of low-complexity linear detectors, a hybrid MIMO detection scheme is developed, which leverages the low-complexity advantage of MMSE detection and the fixed-complexity characteristics of the K-best detection algorithm.

A. Algorithm Description

The proposed algorithm comprises five steps that proceed sequentially. The flowchart in Fig. 1 summarizes the procedure of the algorithm. The detail of each step is described as follows.

Step 1: (MMSE equalization and calculation of post-detection SNR) First, the MMSE detected symbol vector

$\tilde{\mathbf{x}}_{\text{MMSE}} = [\tilde{x}_{\text{MMSE}}^1, \dots, \tilde{x}_{\text{MMSE}}^{M_T}]^T$ is obtained. Then, the post-detection SNR for each layer (symbol) k is derived as [16]

$$\text{SNR}_k = \gamma_0 \frac{1}{[\mathbf{H}^H \mathbf{H} + \gamma_0^{-1} M_T \mathbf{I}_{M_T}]_{k,k}^{-1}} - 1, k = 1, \dots, M_T \quad (7)$$

where $\mathbf{A}_{k,k}^{-1}$ denotes the k th diagonal entry of \mathbf{A}^{-1} and $\gamma_0 = \sigma_x^2 / 2\sigma_v^2$. The entries of the MMSE detected symbol vector are then permuted in descending order of SNR, resulting $\tilde{\mathbf{x}}_{p1} = [\tilde{x}_{\text{MMSE}}^{i_1}, \dots, \tilde{x}_{\text{MMSE}}^{i_{M_T}}]^T$, where $\mathbf{i} = [i_1, \dots, i_{M_T}]^T$ denotes the new indexing. The column vectors $\mathbf{h}_1, \dots, \mathbf{h}_{M_T}$ of \mathbf{H} are permuted accordingly, giving $\mathbf{H}_{p1} = [\mathbf{h}_{i_1}, \dots, \mathbf{h}_{i_{M_T}}]$.

Step 2: (Dividing symbols into groups and P -selection) To facilitate subsequent hybrid detection, the MMSE detected symbol vector is divided into two detection groups, namely a correct-layer group and an error-layer group, according to symbols' reliability. The index vector \mathbf{i} is divided accordingly, i.e., $\mathbf{i} = [(i_1^c, \dots, i_{n_c}^c), (i_1^e, \dots, i_{n_e}^e)]^T$, where n_c and n_e represent the number of elements in each group and $n_c + n_e = M_T$. To provide algorithmic flexibility and further enhance the detection performance, a configurable set of P elements may be selected from the correct-layer group and moved to the error-layer group. This P -selection process essentially changes the group-size pair from (n_c, n_e) to $(n_c - P, n_e + P)$. Note that there are $\binom{n_c}{P}$ such selections. For example, for $P = 1$, the $\binom{n_c}{P} = n_c$ possible combinations and their corresponding indexing are given as follows:

$$\begin{aligned} \mathbf{i}^1 &= [(i_2^c, \dots, i_{n_c}^c), (i_1^c, i_1^e, \dots, i_{n_e}^e)]^T \\ \mathbf{i}^2 &= [(i_1^c, i_3^c, \dots, i_{n_c}^c), (i_2^c, i_1^e, \dots, i_{n_e}^e)]^T \\ &\vdots \\ \mathbf{i}^{\binom{n_c}{P}} &= [(i_1^c, \dots, i_{n_c-P}^c), (i_{n_c-P+1}^c, i_1^e, \dots, i_{n_e}^e)]^T. \end{aligned} \quad (8)$$

Step 3: (Permuting the channel matrix and symbol vector) The columns $\mathbf{h}_{i_1}, \dots, \mathbf{h}_{i_{M_T}}$ of \mathbf{H}_{p1} and the entries of the sorted MMSE detected symbol vector $\tilde{\mathbf{x}}_{p1}$ are permuted according to these $\binom{n_c}{P}$ index vectors, i.e.,

$$\mathbf{H}_{p2} = [\mathbf{h}_{i_1^k}, \dots, \mathbf{h}_{i_{M_T}^k}] \quad (9)$$

$$\tilde{\mathbf{x}}_{p2} = [\tilde{x}_{\text{MMSE}}^{i_1^k}, \dots, \tilde{x}_{\text{MMSE}}^{i_{M_T}^k}]^T \quad (10)$$

where i_j^k is the j th entry of \mathbf{i}^k , and $k = 1, \dots, \binom{n_c}{P}$.

Step 4: (Reduced-dimension K-best detection) Among the two detection groups, the symbols in the error-layer group (corresponding to the last $n_e + P$ symbols of $\tilde{\mathbf{x}}_{p2}$) are more prone to errors and thus an additional procedure is performed on them to yield improved overall detection results. Specifically, an h-best detection algorithm is performed for these $n_e + P$ symbols, and the result will replace the MMSE result to combine with the first $n_c - P$ elements of $\tilde{\mathbf{x}}_{p2}$ to give a solution candidate. The solution candidate is then permuted back according to \mathbf{i}^k to form the vector $\tilde{\mathbf{x}}_{\text{HYB}}^k$. This procedure is repeated $\binom{n_c}{P}$ times, each time producing a $\tilde{\mathbf{x}}_{\text{HYB}}^k$ for a particular permutation \mathbf{i}^k in (8).

Step 5: (Outputting the joint MMSE and h-best detection results) The $\binom{n_c}{P}$ solution candidates $\tilde{\mathbf{x}}_{\text{HYB}}^k$ are collected and the one that yields the minimum $\|\mathbf{y} - \mathbf{H}\tilde{\mathbf{x}}_{\text{HYB}}^k\|^2$ is outputted as the solution of the hybrid detection scheme.

It is worthwhile to note that in the proposed algorithm the K-best algorithm is applied on a reduced-dimension symbol space, since $n_e + P < M_T$. As a result, a smaller K is needed to achieve desirable performance (i.e., h-best algorithm). As long as such a complexity reduction can offset the cost of performing MMSE detection, the proposed algorithm will have some performance and/or complexity advantage over the conventional K-best scheme, as will be verified in Sec. IV.

B. Complexity Evaluation

Here we evaluate the computational complexity of the proposed detection scheme and benchmark schemes in terms of real numerical operations. The complexity of computing $\|\mathbf{y} - \mathbf{H}\mathbf{x}\|^2$ is determined to be $\mathcal{C}_0 = 8M_T^2 + 8M_T - 2$. Complexity evaluations for different schemes are presented below in terms of the size of modulation and system.

- 1) *ML detection:* Since ML detection examines all symbol vectors to find the one that minimizes $\|\mathbf{y} - \mathbf{H}\mathbf{x}\|^2$, its complexity is $\mathcal{C}_{\text{ML}} = |\mathcal{S}|^{M_T} \mathcal{C}_0$.
- 2) *MMSE detection:* By using the Gauss-Jordan Elimination method to calculate matrix inversion, the complexity is $\mathcal{C}_{\text{MMSE}} = (56/3)M_T^3 + 40M_T^2 + (34/3)M_T + 1$.
- 3) *K-best detection:* The complexity of the K-best algorithm is typically evaluated in terms of the number of visited nodes in breadth-first tree search. Since the K-best algorithm maintains K nodes at each layer, the number of visited nodes is $V_{\text{KB}} = |\mathcal{S}| + (M_T - 1) \times |\mathcal{S}| \times K$. Thus, its complexity is given by

$$\mathcal{C}_{\text{KB}} = V_{\text{KB}} \times \mathcal{C}_0. \quad (11)$$

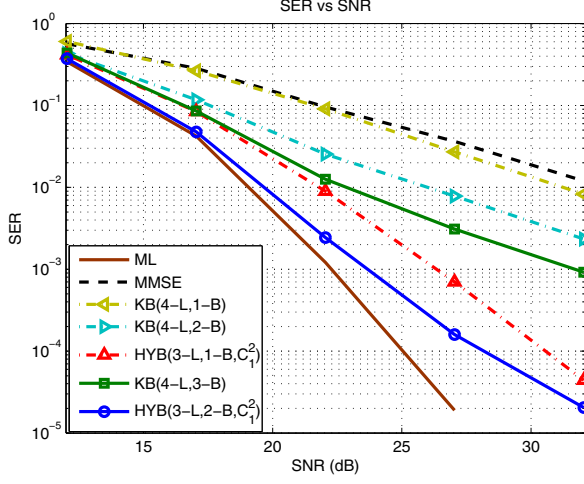
- 4) *Hybrid MMSE and K-best detection:* Given the group-size pair (n_c, n_e) , P -selection, and an h-best algorithm applied to layer $(n_c - P + 1)$ to layer M_T , the number of visited nodes is $V_{\text{HYB}} = \binom{n_c}{P} \times (|\mathcal{S}| + (M_T - n_c + P - 1) \times |\mathcal{S}| \times h)$. The complexity is

$$\mathcal{C}_{\text{HYB}} = V_{\text{HYB}} \times \mathcal{C}_0. \quad (12)$$

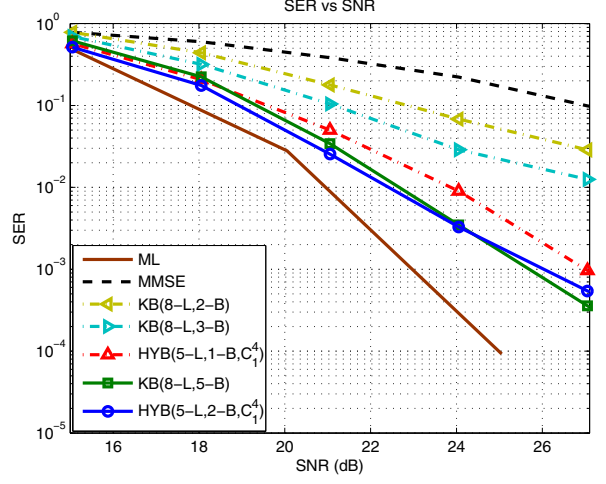
IV. SIMULATION RESULTS

In this section, computer simulation is conducted to understand the performance of the proposed hybrid scheme in comparison with ML detection, MMSE detection, and K-best detection schemes. To conduct a thorough study, four scenarios are considered: 1) 4×4 MIMO with 4-QAM, 2) 8×8 MIMO with 4-QAM, 3) 8×8 MIMO with 16-QAM, and 4) 4×4 MIMO with 64-QAM. In the simulation, the SNR is defined as $\Upsilon = \mathbb{E}[(\mathbf{H}\mathbf{x})^H(\mathbf{H}\mathbf{x})] / \mathbb{E}[\mathbf{v}^H \mathbf{v}]$. We adopt the following legends:

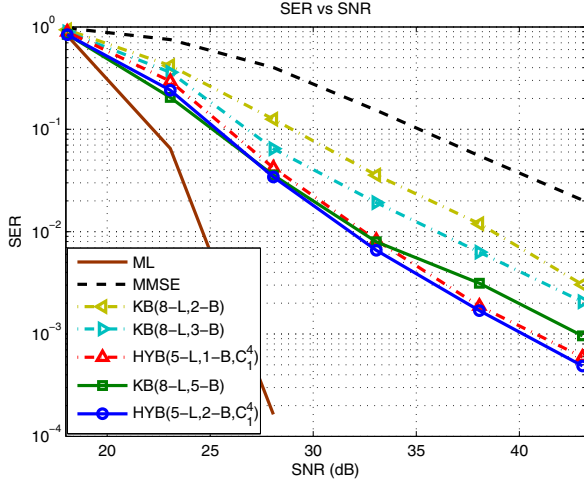
- 1) KB(M -L, K -B) stands for the K-best algorithm performed on M layers.
- 2) HYB(m -L, h -B, $C_P^{n_c}$) stands for the proposed hybrid algorithm with group-size pair (n_c, n_e) , P -selection



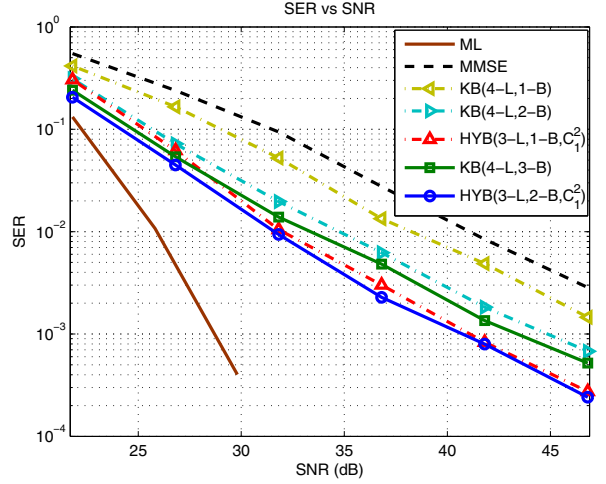
(a) 4×4 , 4-QAM, $(P = 1)$ -selection: $(n_c, n_e) = (2, 2) \Rightarrow (n_c - P, n_e + P) = (1, 3)$ for the hybrid method.



(b) 8×8 , 4-QAM, $(P = 1)$ -selection: $(n_c, n_e) = (4, 4) \Rightarrow (n_c - P, n_e + P) = (3, 5)$ for the hybrid method.



(c) 8×8 , 16-QAM, $(P = 1)$ -selection: $(n_c, n_e) = (4, 4) \Rightarrow (n_c - P, n_e + P) = (3, 5)$ for the hybrid method.



(d) 4×4 , 64-QAM, $(P = 1)$ -selection: $(n_c, n_e) = (2, 2) \Rightarrow (n_c - P, n_e + P) = (1, 3)$ for the hybrid method.

Fig. 2. SER performance of MIMO detection schemes. (a) 4×4 MIMO with 4-QAM modulation. (b) 8×8 MIMO with 4-QAM modulation. (c) 8×8 MIMO with 16-QAM modulation. (d) 4×4 MIMO with 64-QAM modulation.

$(P \leq n_c)$, and the h-best algorithm ($h \leq K$) performed $C_P^{n_c} = \binom{n_c}{P}$ times on m layers ($m \leq M$).

A. Parameter Setting

In order to conduct a fair performance comparison, different schemes are normalized in terms of their computational complexity. Specifically, given a KB(M -L, K -B) scheme, parameters are chosen for HYB(m -L, h -B, $C_P^{n_c}$) so that (11) and (12) are roughly equal to guarantee a fair comparison between our hybrid scheme and the conventional K-best scheme.

B. Results and Discussions

The SER performance of the proposed hybrid scheme is demonstrated for four scenarios in Figs. 2(a)–2(d). P -selection with $P = 1$ is considered for all scenarios.

In Fig. 2(a), based on the rationale stated in Sec. IV-A, we compare HYB(3-L, 1-B, C_1^2) with KB(4-L, 1-B) and KB(4-L, 2-B) (since equating (11) and (12) gives a $K \approx 1.67$ in this case), and HYB(3-L, 2-B, C_1^2) with KB(4-L, 3-B). It is seen in Fig. 2(a) that HYB(3-L, 1-B, C_1^2) outperforms KB(4-L, 2-B) by about 4 dB, and outperforms KB(4-L, 1-B) and MMSE by about 10 dB at $\text{SER} = 10^{-2}$. On the other hand, HYB(3-

L, 2-B, C_1^2) outperforms KB(4-L, 3-B) by about 8 dB and is only 1.5 dB short of ML at $\text{SER} = 10^{-3}$. The advantage of the hybrid scheme over conventional MMSE or K-best alone is remarkable in this scenario.

In Fig. 2(b), we compare HYB(5-L, 1-B, C_1^4) with KB(8-L, 2-B) and KB(8-L, 3-B), and HYB(5-L, 2-B, C_1^4) with KB(8-L, 5-B). It is seen that HYB(5-L, 1-B, C_1^4) outperforms its K-best counterparts by about 4 dB at $\text{SER} = 10^{-2}$, while HYB(5-L, 2-B, C_1^4) achieves similar performance as KB(8-L, 5-B). It is also observed that in high SNR regime KB(8-L, 2-B) and KB(8-L, 3-B) start to experience the error-floor effect whereas the proposed HYB(5-L, 1-B, C_1^4) seems more unaffected by it.

In Fig. 2(c), the same comparison pairs as in Fig. 2(b) are established. It is seen again that the proposed hybrid schemes outperform K-best and MMSE detectors. Interestingly, HYB(5-L, 2-B, C_1^4) demonstrates comparable performance as HYB(5-L, 1-B, C_1^4) despite a larger value of h used. This is because in this scenario (large MIMO with higher-order modulation), the performance of the proposed hybrid scheme is limited by the MMSE detection performance and therefore increasing h in the h-best algorithm provides little performance gain. To further enhance the performance of the hybrid scheme in this scenario, a larger value of P can be employed to effectively mitigate the MMSE detection error, at the cost of higher computational complexity.

In Fig. 2(d), the same comparison pairs as in Fig. 2(a) are established and similar observations can be drawn. In this scenario, however, the performance advantage of the proposed hybrid scheme is smaller as compared to Fig. 2(a). The reason is that higher-order modulation has more complicated decision boundaries which result in performance degradation in MMSE detection and consequently in the proposed method. This can be effectively addressed with a larger P in P -selection, as discussed previously.

V. CONCLUSION

A new MIMO detection scheme concatenating the MMSE detector and K-best algorithm has been proposed in this paper. The proposed scheme partially retains the initial MMSE solution according to the post-detection SNR, and partially initiates a reduced-dimension K-best algorithm to identify improved solutions. In a fair comparison with the conventional K-best algorithm, the proposed hybrid method demonstrates noticeable performance advantage at comparable complexity cost.

REFERENCES

- [1] M. O. Damen, H. E. Gamal, and N. C. Beaulieu, "On maximum-likelihood detection and the search for the closest lattice point," *IEEE Trans. Inform. Theory*, vol. 49, pp. 2372–2388, Oct. 2003.
- [2] K. Wong, C. Tsui, R. Cheng, and W. Mow, "A VLSI architecture of a K-best lattice decoding algorithm for MIMO channels," in *Proc. IEEE International Symposium on Circuits and Systems*, 2002.
- [3] U. Fincke and M. Pohst, "Improved methods for calculating vectors of short length in a lattice, including a complexity analysis," *Mathematics of computation*, vol. 44, no. 170, pp. 463–471, 1985.
- [4] C. Schnorr and M. Euchner, "Lattice basis reduction: Improved practical algorithms and solving subset sum problems," *Mathematical programming*, vol. 66, no. 1, pp. 181–199, 1994.
- [5] Q. Li and Z. Wang, "Improved K-best sphere decoding algorithms for MIMO systems," in *Proc. IEEE International Symposium on Circuits and Systems (ISCAS)*, 2006, pp. 1159–1162.
- [6] S. Mondal, A. Eltawil, and K. Salama, "Architectural optimizations for low-power K-best MIMO decoders," *IEEE Trans. Veh. Tech.*, vol. 58, no. 7, pp. 3145–3153, 2009.
- [7] Z. Guo and P. Nilsson, "Algorithm and implementation of the K-best sphere decoding for MIMO detection," *IEEE J. Select. Areas Commun.*, vol. 24, pp. 491–503, Mar. 2006.
- [8] C. Shen and A. Eltawil, "A radius adaptive K-best decoder with early termination: algorithm and VLSI architecture," *IEEE Transactions on Circuits and Systems I: Regular Papers*, vol. 57, no. 9, pp. 2476–2486, 2010.
- [9] M. McKay and I. Collings, "Capacity and performance of MIMO-BICM with zero-forcing receivers," *IEEE Transactions on Communications*, vol. 53, no. 1, pp. 74–83, 2005.
- [10] S. Yoshizawa, Y. Yamauchi, and Y. Miyana, "A complete pipelined MMSE detection architecture in a 4x4 MIMO-OFDM receiver," in *Proc. IEEE International Symposium on Circuits and Systems (ISCAS)*, 2008, pp. 2486–2489.
- [11] E. Jang, S. Nam, J. Kim, and J. Cioffi, "Improved OSIC decoder for spatially multiplexed system," in *Proc. IEEE International Conference on Communications (ICC)*, vol. 7, 2006, pp. 2963–2968.
- [12] R. Chen, R. Peng, and B. Farhang-Boroujeny, "Markov Chain Monte Carlo: Applications to MIMO detection and channel equalization," in *Proc. IEEE Information Theory and Applications Workshop*, 2009, pp. 44–49.
- [13] M. Rupp, G. Gritsh, and H. Weinrichter, "Approximate ML detection for MIMO systems with very low complexity," in *Proc. IEEE International Conference on Acoustics, Speech, and Signal Processing*, 2004.
- [14] S. M. Kay, *Fundamentals of Statistical Signal Processing: Estimation Theory*. Englewood Cliffs, NJ: Prentice-Hall, 1993.
- [15] G. H. Golub and C. F. Van Loan, *Matrix Computations*, 3rd ed. Baltimore: Johns Hopkins Univ. Press, 1996.
- [16] R. Heath Jr and D. Love, "Multimode antenna selection for spatial multiplexing systems with linear receivers," *IEEE Transactions on Signal Processing*, vol. 53, no. 8, pp. 3042–3056, 2005.